

EDLEMAN

ngth of the
Fig. 4. This
s II and III
nich can be

f Scientific
tion under
rd Univer-
University.
Sherbrooke
e Materials
ence Foun-

977), 101.

ress (1964).

SHEET NECKING-II. TIME-INDEPENDENT BEHAVIOR*

J. W. HUTCHINSON

Harvard University, Cambridge, Massachusetts

K. W. NEALE

Université de Sherbrooke, Sherbrooke, Quebec, Canada

ABSTRACT

Various factors affecting the prediction of limit strains in biaxially-stretched sheets are studied. Time-independent material behavior is assumed, and both the flow theory of plasticity as well as a finite-strain version of deformation theory are considered. A localization-band bifurcation analysis is first carried out. The influence of geometric imperfections is then analyzed using the long-wavelength approximation treated in Part I. We also discuss the predicted forming limit curves and comment on their relation to published experimental data. The main emphasis in this Part, however, is on comparisons between the corresponding predictions of flow theory and deformation theory.

INTRODUCTION

In this second Part, various aspects of localized necking in thin sheets are examined. We restrict attention to *time-independent* material response. A theoretical investigation of this phenomenon was apparently initiated by Hill [1], who considered rigid-plastic solids obeying the common flow theories of plasticity.

Hill's analysis, which is conducted within the framework of generalized plane stress, predicts that localized necking in biaxially stretched sheets only occurs for those principal strain states varying between uniaxial tension and plane strain. However, it is well-established experimentally that necking-type failures take place in the so-called "biaxial tension" range where, since both principal strains are positive, Hill's criterion predicts infinite ductility. Two approaches have been formulated to resolve this discrepancy between Hill's result and experiments. The first approach, due to Marciniak and Kuczyński [2] and extended by Sowerby

* The material in this three-part paper was presented orally in Session II under the title "Constitutive Relations for Sheet Metal" and Session IV under the title "Sheet Necking: Influence of Constitutive Theory and Strain-Rate Dependence."

and Duncan [3], postulates the existence of an initial nonhomogeneity in the form of a narrow band across the sheet. The localization process during straining is then described in terms of the growth of the nonhomogeneity relative to the remainder of the sheet. To examine this hypothesis, Azrin and Backofen [4] conducted a series of experiments on a number of metals under strain states varying from plane strain to equibiaxial tension. For most of the metals tested, they found that the experimental results contradicted the trend of the Marciniak-Kuczyński (M-K) theory. It is important to note, however, that the J_2 (von Mises) flow theory of plasticity was assumed in the analyses.

An alternative approach, recently proposed by Stören and Rice [5], incorporates a J_2 deformation theory of plasticity into a classical bifurcation analysis. The bifurcation mode corresponds to localized deformation in a narrow band, as in Hill's analysis [1]. In certain cases, the results with this theory showed much better agreement with experimental trends than those obtained with the M-K flow theory analysis.

These developments in sheet necking analysis closely parallel discussions which have taken place in the related field of plastic buckling. There, much attention was focused on the reliability of J_2 deformation theory bifurcation predictions vs. the severe imperfection-sensitivity often associated with J_2 flow theory calculations. In spite of many objections which were initially raised concerning the use of deformation theory, it was later shown that use of this theory could be rigorously justified in bifurcation analyses since it is equivalent to a flow theory which permits the development of yield-surface corners (see discussion in [6]). The fact that bifurcation calculations based on deformation theory are generally in much better accord with experimentally determined buckling loads than the corresponding flow theory predictions has strongly favored the use of deformation theory in this application. On the other hand, it has also been demonstrated that incorporation of realistic imperfections in a J_2 flow theory analysis usually produces buckling loads which agree adequately with test data. Consequently, it is still an open question as to which is the more fundamental approach to analyzing plastic buckling.

This Part of our study represents an extensive investigation into various factors which affect necking in thin sheets. The main emphasis throughout is on comparisons between the theoretical predictions of flow theory and deformation theory of plasticity. A finite-strain version of J_2 deformation theory, somewhat different than that proposed by Stören and Rice [5], is introduced and applied to both a bifurcation analysis and an assessment of imperfection-sensitivity. The imperfection-sensitivity analysis is based on the "long-wavelength" approximation treated in detail in Part I of this paper. We consider the full biaxial stretching range, i.e., with principal strain states varying between uniaxial and equibiaxial tension, and obtain corresponding results according to J_2 flow theory.

An important feature of sheet necking is seen to be the imperfection-sensitivity associated with the deformation theory as well as with the flow theory. This is in sharp contrast to plastic buckling results obtained using deformation theory, which are often relatively insensitive to imperfections. In the discussion of such

SHEE

result
theor

CON:

In
theor
is as J_2 Fl
to fix

wher

Here
Jaun
 f is
any
to d.

whe

Her
stre
stre
It
plar
bifu
and
 $\bar{\sigma}_{33}$
plas

Ref

results and relevant experimental data, we address the issue of deformation theory vs. flow theory in this context.

CONSTITUTIVE LAWS

In this study finite-strain versions of both J_2 flow theory and J_2 deformation theory of plasticity will be employed. Throughout this investigation the material is assumed to be incompressible and initially isotropic.

J_2 Flow Theory—For the flow theory analysis the constitutive law, with reference to fixed Cartesian coordinates, is taken to be (see for example [7-9])

$$\dot{\epsilon}_{ij} = \frac{3}{2E} \bar{s}_{ij} + \frac{\alpha f}{E} s_{ij} s_{kl} \bar{s}_{kl} \quad (1)$$

where for incipient yielding

$$\begin{aligned} \alpha &= 1 & \text{if } J_2 = s_{ij} \bar{s}_{ij} \geq 0 \\ \alpha &= 0 & \text{if } J_2 < 0 \end{aligned} \quad (2)$$

Here, $\dot{\epsilon}_{ij}$ is the Eulerian strain-rate tensor, E is Young's modulus, \bar{s}_{ij} denotes the Jaumann rate of change of the Cauchy stress deviator $s_{ij} = \sigma_{ij} - \frac{1}{3} \delta_{ij} \sigma_{kk}$, and f is a function of $J_2 (= \frac{1}{2} s_{ij} s_{ij})$ which can be chosen to make (1) coincide with any monotonic proportional loading history. If the uniaxial tension curve is used to determine f , the inverted form of (1) for plastic loading becomes

$$\bar{\sigma}_{ij} = \frac{2E}{3} [\dot{\epsilon}_{ij} - Q s_{ij} s_{kl} \dot{\epsilon}_{kl}] + \delta_{ij} \dot{p} \quad (3)$$

where p is the hydrostatic pressure, and

$$Q = \frac{3}{2\sigma_e^2} \left(1 - \frac{E_t}{E} \right) \quad (4)$$

Here, the tangent modulus E_t is regarded as a function of the effective stress $\sigma_e (= \sqrt{3J_2})$ and in simple tension corresponds to the slope of the true stress-natural (logarithmic) strain curve.

In the localization-band bifurcation analysis, the assumption of approximate plane stress will be adopted. The state of uniform stress considered prior to bifurcation is such that the only nonvanishing stress components are $\sigma_{11} \equiv \sigma_1$ and $\sigma_{22} \equiv \sigma_2$. In this case, \dot{p} can be eliminated from (3) by means of the relation $\bar{\sigma}_{33} = 0$ and the incompressibility condition $\dot{\epsilon}_{kk} = 0$. The constitutive law (3) for plastic loading then reduces to

$$\begin{aligned} \bar{\sigma}_1 &= \hat{L}_{11} \dot{\epsilon}_1 + \hat{L}_{12} \dot{\epsilon}_2 \\ \bar{\sigma}_2 &= \hat{L}_{12} \dot{\epsilon}_1 + \hat{L}_{22} \dot{\epsilon}_2 \\ \bar{\sigma}_{12} &= 2\hat{L}_s \dot{\epsilon}_{12} \end{aligned} \quad (5)$$

References pp. 149-150.

where the flow theory instantaneous moduli are given by

$$\begin{aligned}\hat{L}_{11} &= \frac{4}{3}E - (E - E_t) \left(\frac{\sigma_1}{\sigma_e} \right)^2 \\ \hat{L}_{22} &= \frac{4}{3}E - (E - E_t) \left(\frac{\sigma_2}{\sigma_e} \right)^2 \\ \hat{L}_{12} &= \frac{2}{3}E - (E - E_t) \frac{\sigma_1 \sigma_2}{(\sigma_e)^2} \\ \hat{L}_s &= \frac{E}{3}\end{aligned}\quad (6)$$

J_2 Deformation Theory—To construct a finite-strain version of the deformation theory constitutive law, we make use of Hill's theory [10] for finitely deformed isotropic elastic solids. Because of isotropy, the principal directions of Cauchy stress must coincide with the axes of the Eulerian strain ellipsoid. Furthermore, the state of strain in a material element is completely specified by the three principal stretches ($\lambda_1, \lambda_2, \lambda_3$) relative to some reference configuration, together with the principal directions of strain. "Principal axes techniques" introduced by Hill [10] can then be conveniently applied to determine the deformation theory instantaneous moduli analogous to (6). Such principal axes methods will also prove to be convenient for the direct finite deformation calculation performed in a subsequent Section on Long-wavelength Analysis.

The most appropriate measure of strain in our formulation seems to be the logarithmic strain tensor which, by definition, is coaxial with the Lagrangian strain ellipsoid and has principal values

$$\epsilon_i = \ln \lambda_i \quad (7)$$

In [10, 11] Hill has presented convincing arguments in favor of this measure. For our purposes we simply note that since $\dot{\epsilon}_i = \dot{\lambda}_i/\lambda_i$ with (7) the incompressibility constraint $\lambda_1\lambda_2\lambda_3 = 1$ becomes exactly $\epsilon_{ii} = 0$ as well as $\dot{\epsilon}_{ii} = 0$.

In view of the above remarks, the well-known small strain J_2 deformation theory can immediately be extended to finite strains as follows

$$\epsilon_i = \mu s_i \quad (8)$$

where μ is assumed to be a function of the effective stress $\sigma_e = (3s_i s_i/2)^{1/2}$ or the effective strain $\epsilon_e = (2\epsilon_i \epsilon_i/3)^{1/2}$, obtainable from the uniaxial tension curve. Since σ_e and ϵ_e are respectively equal to the true stress and true strain in uniaxial tension,

$$\mu = \frac{3}{2} \frac{\epsilon_e}{\sigma_e} = \frac{3}{2E_s} \quad (9)$$

in which E_s denotes the secant modulus. (Note that $\bar{\epsilon}$ rather than ϵ_e will be used to denote effective strain in the flow theory analysis. This is defined as $\int d\bar{\epsilon}$ where $d\bar{\epsilon} = (2d\epsilon_{ij}d\epsilon_{ij}/3)^{1/2}$. For monotonic proportional straining paths $\epsilon_e = \bar{\epsilon}$.)

In terms of
(8) becomes

For a true st

equation (10

where the st

Although
our long-wa
band bifurc
stress and s

When this i
(5), the def

These relat
(6). Hill's f

A finite-
Stören and
only when
relative to

References

In terms of the principal components of Cauchy stress, the constitutive law (8) becomes

$$\sigma_i = \frac{2}{3} E_s \epsilon_i - p \quad (10)$$

For a true stress-natural strain curve of the form

$$\begin{aligned} \sigma_e &= K \epsilon_e^N && \text{(deformation theory)} \\ \sigma_e &= K \bar{\epsilon}^N && \text{(flow theory)} \end{aligned} \quad (11)$$

equation (10) can also be expressed as follows (c.f. [12])

$$\sigma_i = \lambda_i \frac{\partial W}{\partial \lambda_i} - p \quad \text{(no sum on } i) \quad (12)$$

where the strain energy density function W is given by

$$W = \frac{K}{N+1} \epsilon_e^{N+1} \quad (13)$$

Although the "total" form (10) of the deformation theory will be employed in our long-wavelength analysis, a rate form of (10) is required for the localization-band bifurcation analysis. From (9) and the conventional definitions of effective stress and strain, the rate form of (10) becomes

$$\begin{aligned} \dot{s}_i &= \dot{\sigma}_i + \dot{p} \\ &= \frac{2}{3} E_s \dot{\epsilon}_i - s_i (E_s - E_t) \frac{s_k \dot{\epsilon}_k}{(\sigma_e)^2} \end{aligned} \quad (14)$$

When this is specialized to the plane stress case considered in the derivation of (5), the deformation theory instantaneous moduli corresponding to (σ_{1-3}) are

$$\begin{aligned} \hat{L}_{11} &= \frac{4}{3} E_s - (E_s - E_t) \left(\frac{\sigma_1}{\sigma_e} \right)^2 \\ \hat{L}_{22} &= \frac{4}{3} E_s - (E_s - E_t) \left(\frac{\sigma_2}{\sigma_e} \right)^2 \\ \hat{L}_{12} &= \frac{2}{3} E_s - (E_s - E_t) \frac{\sigma_1 \sigma_2}{(\sigma_e)^2} \end{aligned} \quad (15)$$

These relations also follow from a substitution of the secant modulus E_s for E in (6). Hill's formula [10] for the instantaneous shear modulus gives

$$2\hat{L}_s = \frac{\lambda_1^2 + \lambda_2^2}{\lambda_1^2 - \lambda_2^2} (\sigma_1 - \sigma_2) = \frac{2}{3} E_s \ln \left(\frac{\lambda_1}{\lambda_2} \right) \frac{\lambda_1^2 + \lambda_2^2}{\lambda_1^2 - \lambda_2^2} \quad (16)$$

A finite-strain version of J_2 deformation theory has recently been proposed by Stören and Rice [5] which, as discussed by these authors, has path independence only when the strains are small or when the principal axes of strain are fixed relative to the material. If the principal axes are fixed relative to the material the

References pp. 149-150.

present deformation theory and that of Stören and Rice coincide in relating stress to strain. For proportional loading, which in the present study corresponds to monotonically increasing ϵ_1 and ϵ_2 in fixed ratio, the two deformation theories and the flow theory (3) all coincide. Only the present deformation theory is independent of the loading path for arbitrary histories. According to the theory of [5] the instantaneous shear modulus, instead of (16), is $2\hat{L}_s = 2E_s/3$, whereas the remaining moduli are given still by (15). For equibiaxial stretching ($\lambda_1 = \lambda_2$) the instantaneous shear modulus \hat{L}_s from (16) does coincide with the Stören-Rice value. However for the strain levels and ratios of interest here, spanning equibiaxial and uniaxial, the value of \hat{L}_s from (16) exceeds the value $E_s/3$ used by Stören and Rice. Since indirect evidence in the range of small strains suggests that deformation theory tends to underestimate the instantaneous moduli of an actual metal when they differ substantially from those of simple flow theory, it can be argued perhaps that the present "true" deformation theory is sufficiently conservative in its estimate of \hat{L}_s in the large strain range.

If the proportional straining path

$$\frac{\epsilon_2}{\epsilon_1} = \rho = \text{const} \quad (17)$$

is imposed on the sheet, then from (1) or (8)

$$\frac{\sigma_1}{\sigma_e} = \frac{2 + \rho}{[3(1 + \rho + \rho^2)]^{1/2}} \quad (18)$$

$$\frac{\sigma_2}{\sigma_e} = \frac{1 + 2\rho}{[3(1 + \rho + \rho^2)]^{1/2}}$$

which can be substituted in the moduli expressions (6) or (15). Furthermore, for power-law hardening of the type (11) in the plastic range

$$E_t = NK\epsilon_e^{N-1}, \quad E_s = K\epsilon_e^{N-1} \quad (19)$$

where

$$\epsilon_e = \bar{\epsilon} = \frac{2(1 + \rho + \rho^2)^{1/2}}{\sqrt{3}} \epsilon_1 \quad (20)$$

LOCALIZATION-BAND BIFURCATION ANALYSIS

The localization-band bifurcation analysis is carried out within the context of plane stress. The analysis is similar to those performed by Hill and Hutchinson [13] and Stören and Rice [5] in that conditions are determined for which the bifurcation mode corresponds to localized plastic deformation in a narrow band while the deformation remains homogeneous elsewhere.

We consider a thin flat sheet which is currently of uniform thickness and subjected to the homogeneous stress field (Fig. 1)

$$\begin{aligned} \sigma_{11} &= \sigma_1, & \sigma_{22} &= \sigma_2 \\ \text{all other} & & \sigma_{ij} &= 0 \end{aligned} \quad (21)$$

Furthermore σ_1 ratio being
The velocity across the band

where v_i denotes the velocity outside the band normal to the band

and the strain

Equilibrium nominal traction denoting the band

From the Cauchy stress

and the condition becomes

References p.

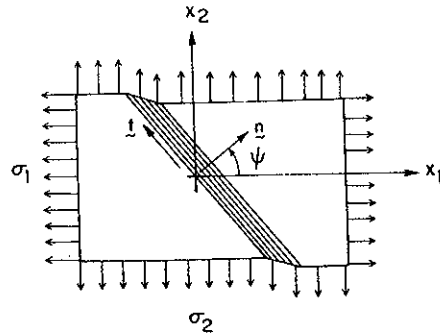


Fig. 1. Localization-band geometry.

Furthermore, we assume proportional loading up to the current state with the σ_2/σ_1 ratio being given by (18).

The velocity field describing the bifurcation mode is constrained to vary only across the band, i.e., [5]

$$v_i = F_i(n_1 x_1 + n_2 x_2) \quad i = 1, 2 \quad (22)$$

where v_i denotes the differences between the velocity components inside and outside the band, and $n_1 = \cos \psi$ and $n_2 = \sin \psi$ are the components of the unit normal to the band. The velocity gradients corresponding to (22) are

$$v_{i,j} = F_i' n_j \equiv g_i n_j \quad i, j = 1, 2 \quad (23)$$

and the strain-rate field is given by

$$\begin{aligned} \dot{\epsilon}_{ij} &= \frac{1}{2}(v_{i,j} + v_{j,i}) \quad i, j = 1, 2 \\ \dot{\epsilon}_{33} &= -(\dot{\epsilon}_{11} + \dot{\epsilon}_{22}) \end{aligned} \quad (24)$$

Equilibrium across the band at the instant of bifurcation requires that the nominal traction-rates \dot{T}_i on the band boundaries be continuous. Thus, with t_{ij} denoting the difference or jump in nominal stress-rates across the boundaries of the band

$$\Delta \dot{T}_j = n_i t_{ij} = 0 \quad (25)$$

From the following relation between nominal stress rates and Jaumann rates of Cauchy stress (for incompressible materials)

$$\dot{t}_{ij} = \dot{\sigma}_{ij} + \sigma_{ik} v_{j,k} - (\sigma_{ik} \dot{\epsilon}_{jk} + \sigma_{jk} \dot{\epsilon}_{ik}) \quad (26)$$

and the constitutive law (5), the condition (25) for the above bifurcation mode becomes

$$\begin{aligned} &\{n_1^2(\hat{L}_{11} - \sigma_1) + n_2^2[\hat{L}_s + \frac{1}{2}(\sigma_2 - \sigma_1)]\}g_1 \\ &+ n_1 n_2\{\hat{L}_{12} + \hat{L}_s - \frac{1}{2}(\sigma_1 + \sigma_2)\}g_2 = 0 \\ &n_1 n_2\{\hat{L}_{12} + \hat{L}_s - \frac{1}{2}(\sigma_1 + \sigma_2)\}g_1 \\ &+ \{n_1^2[\hat{L}_s + \frac{1}{2}(\sigma_1 - \sigma_2)] + n_2^2(\hat{L}_{22} - \sigma_2)\}g_2 = 0 \end{aligned} \quad (27)$$

References pp. 149-150.

In general, simple expressions such as (30) and (31) cannot be obtained with the present deformation theory, so numerical solutions of (28) are required to determine the value ψ^* which minimizes the bifurcation strain ϵ_1^* . However, in the so-called "biaxial tension range" ($\rho \geq 0$), $\psi^* = 0$ is the minimizing angle and

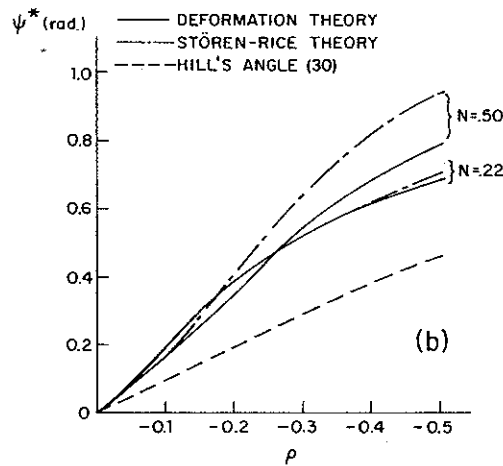
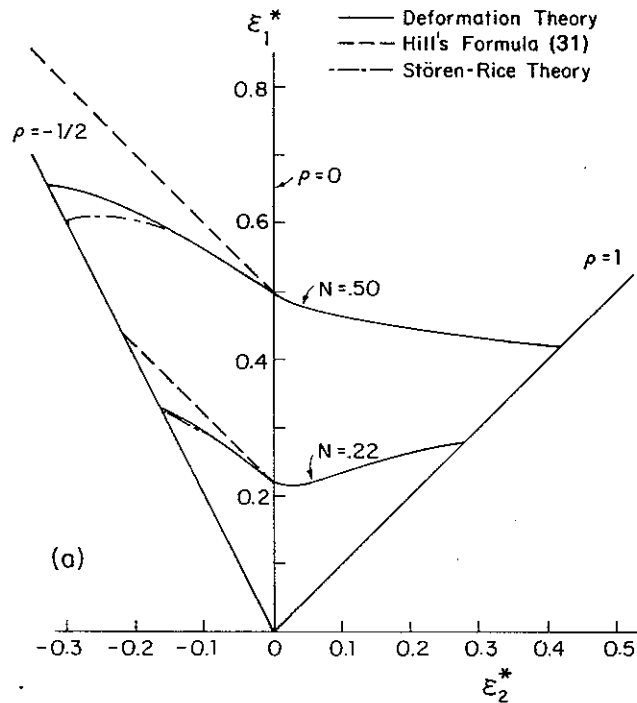


Fig. 2. (a) Forming limit curves from bifurcation analysis for various plasticity theories. (b) Localization-band angle ψ^* in negative- ρ range.

References pp. 149-150.

the critical condition (28) reduces to $n_2 = g_2 = 0$ and $\sigma_1^* = \hat{L}_{11}$, i.e.,

$$\epsilon_1^* = \frac{3\rho^2 + N(2 + \rho)^2}{2(2 + \rho)(1 + \rho + \rho^2)} \quad (32)$$

The principal axes of strain do not rotate for the associated bifurcation mode and the shear modulus \hat{L}_s does not enter into (32) so that, as expected, this result is identical to that obtained by Stören and Rice [5]. In the negative ρ range, however, principal axes do not remain fixed at bifurcation and the present deformation theory leads to results which differ somewhat from those furnished by the Stören-Rice deformation theory.

In Fig. 2(a) the theoretical localization-band bifurcation strains are plotted as "forming limit curves", i.e., curves which illustrate the dependence of the critical strain ϵ_1^* on imposed strain ratio. Here, the solid and dashed curves refer to the deformation theory and flow theory predictions, respectively. Results are shown for a strain hardening exponent $N = .22$, typical of certain steels and aluminum alloys [4, 14], and also $N = .50$ which is representative of brass [15].

In the biaxial tension range ($\rho \geq 0$) only deformation theory predicts bifurcation, as mentioned earlier, and the corresponding necking strains are given by (32). However, Hill's flow theory formula (31) does predict localized necking in the negative ρ range. In this range, the forming limit curves of Fig. 2(a) obtained from (28) with the present version of deformation theory are observed to lie below Hill's curve, yet above the curves furnished by the Stören-Rice deformation theory [5]. The discrepancy between the two deformation theories increases with increasing strain-hardening exponent N . Nevertheless, the discrepancy even for $N = 0.50$ is not very large, and thus the choice of which deformation theory to use may not be critical in this application.

The critical angle ψ^* minimizing the bifurcation strains ϵ_1^* are plotted in Fig. 2(b) for strain ratios varying from plane strain ($\rho = 0$) to uniaxial tension ($\rho = -\frac{1}{2}$). According to flow theory this angle, given by (30), only depends on ρ . With deformation theory the critical orientation also depends on N , and the curves for ψ^* are above Hill's curve. The present version of deformation theory gives values of ψ^* which are between (30) and the predictions of Stören and Rice [5], and fairly close to the latter results for smaller N .

LONG-WAVELENGTH (M-K) ANALYSIS

In order to assess the effects of geometric nonuniformities on localized necking behavior, the "long-wavelength" approximation discussed in Part I will be applied. Consistent with the bifurcation analysis of the preceding section, our approach is within the framework of generalized plane stress. The present analysis is thus along the lines of that introduced by Marciniak and Kuczyński [2] for this problem; however, it is not restricted to the biaxial tension range ($\rho \geq 0$, $\psi = 0$) and both flow theory and deformation theory are employed.

We consider a sheet having a nonuniformity in the form of a groove or band which is initially inclined at an angle ψ (Fig. 3). The thickness along the minimum section in the groove is denoted by $h(t)$, with an initial value $h(0)$. In applying

 σ_1^0

the long-wave thickness ratio section, has a nonuniformity

Throughout the associated with this symbol w

In addition axes are used ψ , and axes x_1

As in the h on the edges

The $x_1 - x_2$ the uniform strain, we ob

The rotation

According cross-section components and t denotir

References pp

(32)

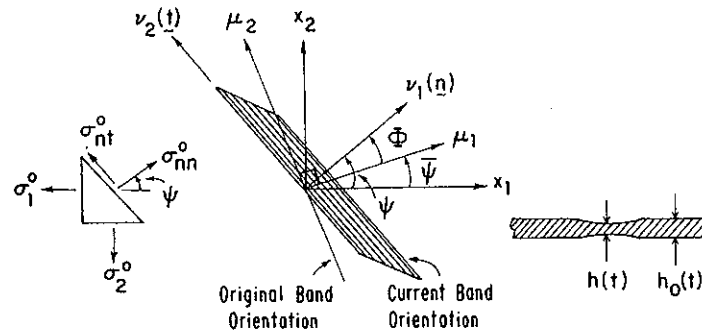


Fig. 3. Conventions for long-wavelength analysis.

the long-wavelength approximation it is tacitly assumed that the band width-to-thickness ratio is large. The region outside the band, referred to as the "uniform" section, has thickness $h_o(t)$ with an initial value $h_o(0)$. The initial geometric nonuniformity is defined as follows

$$\xi = \frac{h_o(0) - h(0)}{h_o(0)} \geq 0 \quad (33)$$

Throughout the analysis a subscript or superscript o will denote quantities associated with behavior in the uniform region of the sheet whereas the absence of this symbol will refer to quantities along the minimum section of the groove.

In addition to the fixed $x_1 - x_2$ reference axes, two other systems of Cartesian axes are used: the set $\mu_1 - \mu_2$ aligned with the initial inclination of the groove $\bar{\psi}$, and axes $\nu_1 - \nu_2$ coincident with the current orientation of the groove ψ .

As in the localization-band bifurcation analysis, we take the loading imposed on the edges of the sheet to be such that

$$\frac{\epsilon_2^o}{\epsilon_1^o} = \rho = \text{const}, \quad \frac{\sigma_2^o}{\sigma_1^o} = \frac{1 + 2\rho}{2 + \rho} \quad (34)$$

The $x_1 - x_2$ axes thus represent the principal directions of stress and strain for the uniform sections of the sheet. From the basic definition (7) of logarithmic strain, we obtain the following relation for the current groove inclination

$$\tan \psi = \frac{\lambda_1^o}{\lambda_2^o} \tan \bar{\psi} = \exp[(1 - \rho)\epsilon_1^o] \tan \bar{\psi} \quad (35)$$

The rotation of the band during loading is thus

$$\Phi = \psi - \bar{\psi} \quad (36)$$

According to the long-wavelength simplification the state of stress over each cross-section is considered to be uniform. That is, we take the stress and strain components to be quantities which are averaged through the thickness. With n and t denoting the normal and tangential directions to the current groove incli-

References pp. 149-150.

nation ($n \equiv \nu_1$, $t \equiv \nu_2$), the equilibrium conditions across the band become

$$\sigma_{nn}^o h_o = \sigma_{nn} h, \quad \sigma_{nt}^o h_o = \sigma_{nt} h \quad \text{or} \quad \frac{\sigma_{nt}}{\sigma_{nn}} = \frac{\sigma_{nt}^o}{\sigma_{nn}^o} \quad (37)$$

In the uniform section, the normal and shear stress components with respect to the $n - t$ axes are given by

$$\begin{aligned} \sigma_{nn}^o &= \sigma_1^o \cos^2 \psi + \sigma_2^o \sin^2 \psi \\ \sigma_{tt}^o &= \sigma_1^o \sin^2 \psi + \sigma_2^o \cos^2 \psi \\ \sigma_{nt}^o &= (-\sigma_1^o + \sigma_2^o) \sin \psi \cos \psi \end{aligned} \quad (38)$$

An effective stress-effective strain law of the type (11) together with the first of (37) and the definitions

$$\epsilon_3 = \ln \frac{h}{h(0)}, \quad \epsilon_2^o = \ln \frac{h_o}{h_o(0)} \quad (39)$$

leads to the following expression (c.f. [14]) for deformation theory

$$\frac{\sigma_{nn}^o / \sigma_e^o}{\sigma_{nn} / \sigma_e} = (1 - \xi) \left(\frac{\epsilon_e}{\epsilon_e^o} \right)^N \exp(\epsilon_3 - \epsilon_3^o) \quad (40)$$

where ξ is the initial geometric nonuniformity introduced in (33). The same expression holds for flow theory with $\epsilon_e / \epsilon_e^o$ replaced by $\bar{\epsilon} / \bar{\epsilon}^o$.

Equation (34) and the basic definition of effective stress yields

$$\frac{\sigma_{nn}^o}{\sigma_e^o} = \frac{(\rho + 2) \cos^2 \psi + (2\rho + 1) \sin^2 \psi}{\sqrt{3}(1 + \rho + \rho^2)^{1/2}} \quad (41)$$

Furthermore, the incompressibility condition $\epsilon_1^o + \epsilon_2^o + \epsilon_3^o = 0$ and (20) gives

$$\epsilon_3^o = -\frac{\sqrt{3}(1 + \rho)}{2(1 + \rho + \rho^2)^{1/2}} \epsilon_e^o \equiv -C \epsilon_e^o \quad (42)$$

Note that, since proportional loading occurs in the uniform section, $\epsilon_e^o \equiv \bar{\epsilon}^o$ in this case.

The purpose of the subsequent analysis is to express the remaining quantities in (40), which correspond to the deformation along the groove, in terms of $\bar{\epsilon}$ (or ϵ_e). The resulting relationships will of course depend on whether flow theory or deformation theory is applied. We seek equations relating $\bar{\epsilon}$ to $\bar{\epsilon}^o$ (or ϵ_e to ϵ_e^o). From these relationships we can calculate the development of the groove and the limit strains in the uniform section of the sheet.

J_2 Flow Theory Analysis—In the flow theory analysis the material is assumed to be rigid-plastic. The constitutive law (1) then becomes

$$d\epsilon_{ij} = \frac{3}{2} \frac{d\bar{\epsilon}}{\sigma_e} s_{ij} \quad (43)$$

Using this expression to find σ_u to find

where the appropriate approximation is used. From the condition

the relation

and equations (3) and (4) calculation that

where for the chosen. Here, i

Substitution of (48) then gives

$$(1 - B -$$

where

From (43) and

with

References pp.

Using this expression together with the defining equation for σ_e , one can eliminate σ_u to find

$$\frac{d\epsilon_u}{d\bar{\epsilon}} = \pm \left[1 - \frac{3}{4} \left(\frac{\sigma_{nn}}{\sigma_e} \right)^2 - 3 \left(\frac{\sigma_{nt}}{\sigma_e} \right)^2 \right]^{1/2} \quad (44)$$

where the appropriate sign depends on the orientation of the band.

From the compatibility condition

$$d\epsilon_u = d\epsilon_u^0 \quad (45)$$

the relation

$$d\epsilon_u^0 = d\epsilon_1^0 \sin^2 \psi + d\epsilon_2^0 \cos^2 \psi \quad (46)$$

and equations (34), (37), (38) and (44), it follows after a lengthy but straightforward calculation that

$$\frac{\sigma_{nn}}{\sigma_e} = \frac{1}{AH} \left[1 - B \left(\frac{d\bar{\epsilon}^0}{d\bar{\epsilon}} \right)^2 \right]^{1/2} \quad (47)$$

where for the range $-\frac{1}{2} \leq \rho \leq 1$ considered here the root $\sigma_{nn} > 0$ has been chosen. Here, in a form similar to that in [14],

$$A = \frac{\sqrt{3}}{2}$$

$$B = \frac{3(\sin^2 \psi + \rho \cos^2 \psi)^2}{4(1 + \rho + \rho^2)} \quad (48)$$

$$H = \left\{ 1 + \left[\frac{2(\rho - 1) \sin \psi \cos \psi}{(\rho + 2) \cos^2 \psi + (2\rho + 1) \sin^2 \psi} \right]^2 \right\}^{1/2}$$

Substitution of (41), (42) and (47) into the equilibrium equation (40) together with (48) then gives

$$(1 - B - G)^{1/2} H \left[1 - B \left(\frac{d\bar{\epsilon}^0}{d\bar{\epsilon}} \right)^2 \right]^{-1/2} = (1 - \xi) \left(\frac{\bar{\epsilon}}{\bar{\epsilon}^0} \right)^N \exp(C\bar{\epsilon}^0 + \epsilon_3) \quad (49)$$

where

$$G = \frac{(\rho - 1)^2 \sin^2 \psi \cos^2 \psi}{(1 + \rho + \rho^2)} \quad (50)$$

From (43) and (45)–(47), the following expression is obtained

$$\frac{d\epsilon_3}{d\bar{\epsilon}} = -\frac{A}{H} \left[1 - B \left(\frac{d\bar{\epsilon}^0}{d\bar{\epsilon}} \right)^2 \right]^{1/2} - D \frac{d\bar{\epsilon}^0}{d\bar{\epsilon}} \quad (51)$$

with

$$D = \frac{\sqrt{3}(\sin^2 \psi + \rho \cos^2 \psi)}{4(1 + \rho + \rho^2)^{1/2}} \quad (52)$$

References pp. 149–150.

A straightforward incremental solution of (49) and (51) determines the groove deformation $\bar{\epsilon}$ in terms of the prescribed uniform deformation $\bar{\epsilon}^0$. In the numerical solution, the strain ratio ρ and initial groove angle $\bar{\psi}$ are initially specified. The current groove orientation ψ is updated at each increment using (35). For the case $\bar{\psi} = \psi = 0$, equations (49) and (51) reduce to those given by Marciniak *et al* [14].

J_2 Deformation Theory Analysis—In the deformation theory analysis the total form (10) of the constitutive law is employed together with the principal axes techniques referred to previously. Alternatively, an incremental formulation along lines just given for flow theory could be developed, but we prefer to take full advantage of the total form of the deformation theory.

We first describe the deformation in the groove with respect to the $\mu_1 - \mu_2$ axes (Fig. 3) as follows

$$\begin{aligned}\mu_1 &= \delta\bar{\mu}_1 + \gamma\bar{\mu}_2 \\ \mu_2 &= \eta\bar{\mu}_1 + \phi\bar{\mu}_2\end{aligned}\quad (53)$$

Here, and in the following, a bar denotes the initial coordinates of a material point whereas an un-barred coordinate refers to its current position. For the uniform deformation (34),

$$x_1 = \lambda_1^0 \bar{x}_1, \quad x_2 = \lambda_2^0 \bar{x}_2 \quad (54)$$

which, when referred to the $\mu_1 - \mu_2$ axes, becomes

$$\begin{aligned}\mu_1 &= (\lambda_1^0 \cos^2 \bar{\psi} + \lambda_2^0 \sin^2 \bar{\psi})\bar{\mu}_1 - (\lambda_1^0 - \lambda_2^0) \sin \bar{\psi} \cos \bar{\psi} \bar{\mu}_2 \\ \mu_2 &= -(\lambda_1^0 - \lambda_2^0) \sin \bar{\psi} \cos \bar{\psi} \bar{\mu}_1 + (\lambda_1^0 \sin^2 \bar{\psi} + \lambda_2^0 \cos^2 \bar{\psi})\bar{\mu}_2\end{aligned}\quad (55)$$

Compatibility of deformation on $\bar{\mu}_1 = 0$ then leads to the following "matching" conditions

$$\begin{aligned}\phi &= \lambda_1^0 \sin^2 \bar{\psi} + \lambda_2^0 \cos^2 \bar{\psi} \\ \gamma &= -(\lambda_1^0 - \lambda_2^0) \sin \bar{\psi} \cos \bar{\psi}\end{aligned}\quad (56)$$

(From (35), (36) and (56) it follows that $\gamma/\phi = -\tan \Phi$ as expected. Furthermore it can be shown, by describing the groove and uniform deformations in terms of the current $\nu_1 - \nu_2$ reference axes, that (56) is equivalent to (45) where the Eulerian strain rates $\dot{\epsilon}_{ii}$ are matched along the current groove orientation.)

For the uniform deformation the principal directions of stress and strain are the $x_1 - x_2$ axes. However, from (53) the deformation-gradient matrix $A (A_{ij} = \partial \mu_i / \partial \bar{\mu}_j)$ for the groove behavior is

$$A = \begin{bmatrix} \delta & \gamma \\ \eta & \phi \end{bmatrix} \quad (57)$$

Since the Eulerian strain ellipsoid is coaxial with the principal axes of the left Cauchy-Green matrix AA^T , the orientation $\hat{\theta}$ of these axes relative to the $\mu_1 -$

SHEET NECK

 μ_2 reference s

The orientatio

Now, the p
the principal v

where

and I denotes
stretches are

with

From the co
the plane str
becomeAs mentione
coincide with
straightforwa
ponents with

From the a

References pp

μ_2 reference system is given by

$$\tan 2\hat{\theta} = \frac{2(\delta\eta + \gamma\phi)}{(\delta^2 + \gamma^2) - (\eta^2 + \phi^2)} \quad (58)$$

The orientation with respect to the current $\nu_1 - \nu_2$ axes is, from (36) or Fig. 3

$$\theta = \hat{\theta} - \Phi \quad (59)$$

Now, the principal stretches λ_1, λ_2 for the groove deformation are related to the principal values e_1, e_2 of Green's strain matrix \mathbf{e} as follows

$$e_1 = \frac{1}{2}(\lambda_1^2 - 1), \quad e_2 = \frac{1}{2}(\lambda_2^2 - 1) \quad (60)$$

where

$$\mathbf{e} = \frac{1}{2}(\mathbf{A}^T\mathbf{A} - \mathbf{I}) \quad (61)$$

and \mathbf{I} denotes the unit matrix. In view of (57) and these relations, the principal stretches are

$$\lambda_{1,2} = \frac{1}{\sqrt{2}} [(\delta^2 + \eta^2 + \gamma^2 + \phi^2) \pm R]^{1/2} \quad (62)$$

with

$$R = \{[(\delta^2 + \eta^2) - (\gamma^2 + \phi^2)]^2 + 4(\delta\gamma + \eta\phi)^2\}^{1/2}$$

From the constitutive law (10), the incompressibility constraint $\lambda_1\lambda_2\lambda_3 = 1$ and the plane stress approximation $\sigma_3 = 0$ the principal values of Cauchy stress become

$$\begin{aligned} \sigma_1 &= \frac{2}{3} \frac{\sigma_e}{\epsilon_e} \ln(\lambda_1^2 \lambda_2) \\ \sigma_2 &= \frac{2}{3} \frac{\sigma_e}{\epsilon_e} \ln(\lambda_1 \lambda_2^2) \end{aligned} \quad (63)$$

As mentioned previously, the principal directions of this stress tensor must coincide with those of the Eulerian strain tensor for an isotropic material. A straightforward transformation of (63) therefore provides the required stress components with respect to the current groove axes:

$$\begin{aligned} \sigma_{nn} &= \frac{1}{2}[(\sigma_1 + \sigma_2) + (\sigma_1 - \sigma_2) \cos 2\theta] \\ \sigma_{nt} &= \frac{1}{2}(\sigma_1 - \sigma_2) \sin 2\theta \\ \sigma_{tt} &= \frac{1}{2}[(\sigma_1 + \sigma_2) - (\sigma_1 - \sigma_2) \cos 2\theta] \end{aligned} \quad (64)$$

From the above expressions and the third of (37), we obtain the relation

$$\sin 2\theta \ln \left(\frac{\lambda_1}{\lambda_2} \right) = 3MY \quad (65)$$

in which

$$M = \frac{\sigma_{nt}^0}{\sigma_{nn}^0} = \frac{(\rho - 1) \sin \psi \cos \psi}{(\rho + 2) \cos^2 \psi + (2\rho + 1) \sin^2 \psi} \quad (66)$$

and

$$Y = \ln(\lambda_1 \lambda_2) + \frac{1}{3} \cos 2\theta \ln \left(\frac{\lambda_1}{\lambda_2} \right) \quad (67)$$

Furthermore, the equilibrium equation (40) becomes

$$\frac{(\rho + 2) \cos^2 \psi + (2\rho + 1) \sin^2 \psi}{\sqrt{3}(1 + \rho + \rho^2)^{1/2}} = \frac{(1 - \xi)}{\lambda_1 \lambda_2} \left(\frac{\epsilon_e}{\epsilon_e^0} \right)^N \exp(C\epsilon_e^0) \frac{Y}{\epsilon_e} \quad (68)$$

where, according to the basic definition of effective strain

$$\epsilon_e = \frac{2}{\sqrt{3}} [(\ln \lambda_1)^2 + \ln \lambda_1 \ln \lambda_2 + (\ln \lambda_2)^2]^{1/2} \quad (69)$$

For a prescribed strain ratio ρ , initial groove inclination $\bar{\psi}$, and uniform deformation $\bar{\epsilon}^0$, the corresponding groove deformation described by (53) is determined from (65) and (68) together with the matching conditions (56) for ϕ and γ . The unknown parameters δ and η enter implicitly into (65) and (68) through the expressions (58) for the principal directions of stress, (62) for the principal stretches, (69) for the effective strain and (35)–(36) for the band rotation Φ . A Newton-Raphson technique applied to these equations provides the numerical solution of ϵ_e for given ϵ_e^0 . For convenience, we determined the derivatives required in this method numerically.

For the case $\bar{\psi} = 0$, the above analysis implies that $\Phi = \gamma = \eta = \theta = 0$. Furthermore,

$$\lambda_1 = \delta, \quad \lambda_2 = \phi = \lambda_2^0 \quad (70)$$

Equation (65) is thus identically satisfied and (68) reduces to

$$(1 - B)^{1/2} \left[1 - B \left(\frac{\epsilon_e^0}{\epsilon_e} \right)^2 \right]^{-1/2} = (1 - \xi) \left(\frac{\epsilon_e}{\epsilon_e^0} \right)^N \exp(C\epsilon_e^0 + \epsilon_3) \quad (71)$$

which is similar in form to the result (49) obtained in the flow theory analysis for $\psi = 0$. Here, the expression for ϵ_3 becomes [c.f. (51) for $\psi = 0$]

$$\frac{\epsilon_3}{\epsilon_e} = -A \left[1 - B \left(\frac{\epsilon_e^0}{\epsilon_e} \right)^2 \right]^{1/2} - D \frac{\epsilon_e^0}{\epsilon_e} \quad (72)$$

where A , B , C and D are now constants given by (48), (42) and (52) with $\psi = 0$.

PLANE STRAIN CASE ($\rho = 0$)

Before proceeding to results for a wider range of ρ -values, we shall first consider separately the plane strain case ($\rho = 0$). Here, $\bar{\psi} = \psi = 0$ and the deformation and flow theory predictions coincide.

SHEET NECKING

The critical load or (32) is

Furthermore, take on the flow Equations (51) and (71) reduce

This result is a problem of an axial strain.

A direct numerical typical results: N for an initial indicate the n

This value is corresponding, furthermore, the $= 0$. The dashed is no longer

Fig. 4. D of ϵ_1^0/N for References p

The critical bifurcation strain obtained from the localization-band formulas (31) or (32) is

$$\epsilon_1^* \equiv \epsilon_1^o = N \tag{73}$$

Furthermore, the parameters in the foregoing long-wavelength (M-K) analysis take on the following values: $B = D = G = 0$, $H = 1$ and $A = C = \sqrt{3}/2$. Equations (51) or (72) give $\epsilon_3 = -\sqrt{3}\epsilon_e/2$ as expected, and the expressions (49) and (71) reduce to

$$(\epsilon_1^o)^N \exp(-\epsilon_1^o) = (1 - \xi)\epsilon_1^N \exp(-\epsilon_1) \tag{74}$$

This result is identical to the relation obtained in [16] for the corresponding problem of an axisymmetric bar under uniaxial tension with ϵ_1 identified as the axial strain.

A direct numerical solution of the transcendental equation (74) furnishes the typical results shown in Fig. 4, where curves of ϵ_1/ϵ_1^o are plotted against ϵ_1^o/N for an initial geometric nonuniformity $\xi = .005$. The solid dots on these curves indicate the maximum value of ϵ_1^o , which, from (74), is given by

$$\frac{\epsilon_1^o}{N} \exp \left[- \left(\frac{\epsilon_1^o}{N} - 1 \right) \right] = (1 - \xi)^{1/N} \tag{75}$$

This value is attained when the strain in the groove satisfies $\epsilon_1 = N$ and the corresponding x_1 -load component applied to the sheet reaches a maximum. Furthermore, the classical result (73) is retrieved from (75) when the imperfection $\xi = 0$. The dashed portion of each curve in Fig. 4 is also obtained from (74), but is no longer strictly valid since elastic unloading should occur in the uniform

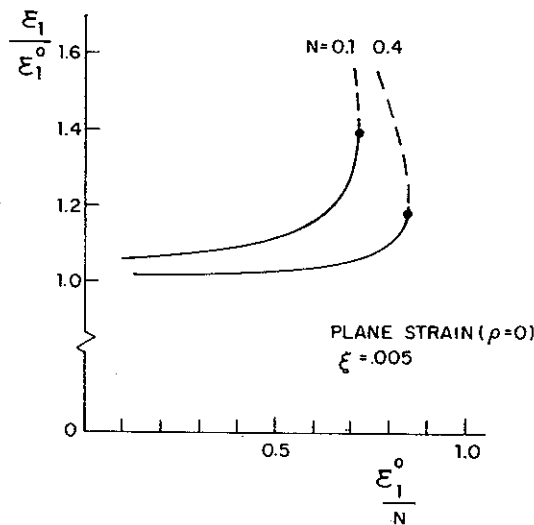


Fig. 4. Development of ratio of strain in neck ϵ_1 to strain outside neck ϵ_1^o as a function of ϵ_1^o/N for plane strain.

References pp. 149-150.

region but has not been taken into account. The important point, however, is that ϵ_1^{0*} given by (75) does correctly give the maximum value of the strain attained in the uniform part of the sheet in the long-wavelength approximation. We therefore refer to this limiting value of uniform strain as the "limit" strain or critical strain for localized necking as it represents the state where the deformation becomes concentrated in the groove while the remainder of the sheet begins to unload. This criterion, which in general is equivalent to $d\bar{\epsilon}^o/d\bar{\epsilon} = 0$ (or $d\epsilon_e^o/d\epsilon_e = 0$) has been discussed in [14, 16]. It will also serve as our definition of critical strain for the other values of strain ratio ρ .

In Fig. 5 the critical strains (75) are plotted against the initial imperfection ξ for strain-hardening exponent values $N = 0.1$ and 0.4 . The dashed curves shown here correspond to the asymptotic result from (75) for small ξ

$$\frac{\epsilon_1^{0*}}{N} = 1 - \sqrt{\frac{2\xi}{N}} \tag{76}$$

It is clear from this expression and Fig. 5 that a small amount of geometric nonuniformity ξ substantially reduces the critical strain for necking. This type of behavior has received considerable attention in connection with the elastic and elastic-plastic buckling of structures, and is characteristic of structures which are referred to as *imperfection-sensitive*. In fact, the $\sqrt{\xi}$ -type dependence indicated in (76) typifies some of the most imperfection-sensitive shell structures [17].

We emphasize again that flow theory and deformation theory give identical results for this case, so imperfection-sensitivity here is not the anomalous im-

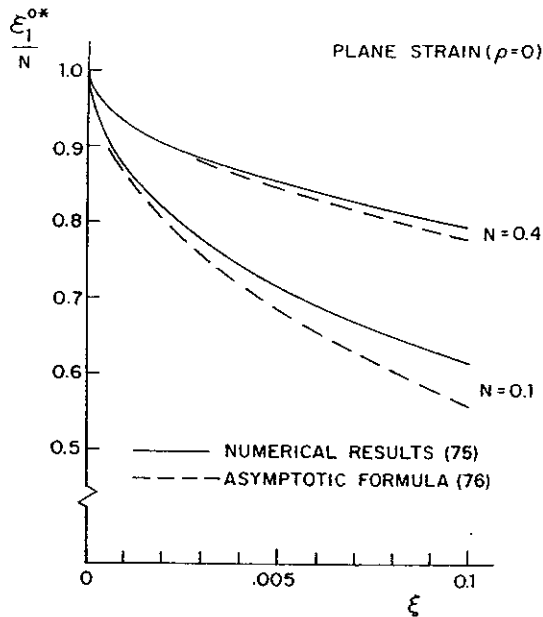


Fig. 5. Imperfection-sensitivity of limit strain ϵ_1^{0*} outside neck.

perfection-sensitive predictions of the theory, as will be

RESULTS AND

The long-wave strain ratios vary with tension, respectively in the long-wavelength limit in the x_2 -direction

The effect of deformation theory is depicted in Fig. 6. The necking strain is also seen to be nonuniformity. The strains are some corresponding d

The discrepancy in tension case. He flow theory as t strain for $\xi = 0$

Fig. 6. Comparison theory and

perfection-sensitivity associated with simple flow theory when the bifurcation predictions of the flow theory are greatly in excess of those for deformation theory, as will be seen to be the case when $\rho > 0$.

RESULTS AND DISCUSSION FOR FULL RANGE OF ρ

The long-wavelength analysis was applied to generate numerical results for strain ratios varying from $\rho = -\frac{1}{2}$ to 1, corresponding to uniaxial and equibiaxial tension, respectively. For $\rho < 0$, various initial band orientations ψ were considered in the long-wavelength analysis to determine the angle which produced the minimum limit strain. For $\rho \geq 0$, the critical angle is such that the band is aligned in the x_2 -direction, i.e., normal to the direction of maximum principal strain ϵ_1^0 .

The effect of the initial geometric nonuniformity ξ on the limit strain ϵ_1^{0*} is depicted in Fig. 6 for $\rho = -\frac{1}{2}, 0, 1$ and $N = .22$. Again, solid curves represent deformation theory results and dashed lines refer to flow theory. As discussed in the previous Section, the plane strain ($\rho = 0$) results here coincide for both theories and exhibit the type of imperfection-sensitivity characterized by (76). The necking strains for uniaxial tension ($\rho = -\frac{1}{2}$) and equibiaxial tension ($\rho = 1$) are also seen to be reduced considerably in the presence of a small geometric nonuniformity. For the uniaxial tension case, the predicted flow theory limit strains are somewhat higher and slightly more imperfection-sensitive than the corresponding deformation theory necking strains.

The discrepancy between the two theories is more drastic for the equibiaxial tension case. Here, there is an enormous imperfection-sensitivity associated with flow theory as the bifurcation analysis in this case predicts an infinite necking strain for $\xi = 0$. Moreover, these flow theory limit strains continue to diminish

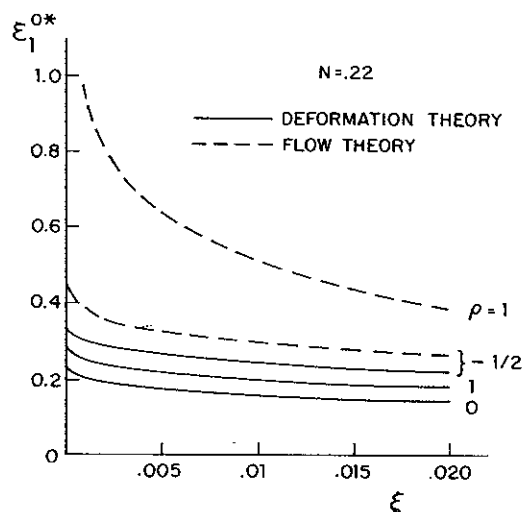


Fig. 6. Comparisons of imperfection-sensitivity of limit strain outside neck for deformation theory and flow theory for three states.

References pp. 149-150.

substantially as ξ increases beyond the value .01. On the other hand, the deformation theory critical strains for $\rho = 1$ do not show this severe sensitivity to the assumed value of ξ since a finite bifurcation strain ($\xi = 0$) exists according to this theory. In contrast to the flow theory results, these limit strains are rather insensitive to variations in ξ within the range .01-.02.

Figs. 7(a) and 7(b) illustrate the manner in which the limit strain ϵ_1^{0*} varies with the initial groove orientation $\bar{\psi}$ and current groove inclination ψ^* at necking. These results correspond to a strip under uniaxial tension ($\rho = -1/2$) with $N = .22$ and initial imperfections $\xi = .01, .001$. In these figures the numerical values $\bar{\psi}_D^*$ and $\bar{\psi}_F^*$ denote the initial orientations, calculated from (35), that would align with the current critical angles ψ_D^* and ψ_F^* predicted by the bifurcation analyses. Here, subscripts *D* and *F* refer to deformation and flow theory, respectively.

The results shown in these figures indicate that the flow theory limit strains are very sensitive to variations in $\bar{\psi}$ and ψ^* , whereas the deformation theory necking strains are relatively insensitive. It can also be seen from these curves that, as the initial imperfection decreases, the angles $\bar{\psi}$ and ψ which minimize ϵ_1^{0*} approach their corresponding values at bifurcation and, even for imperfec-

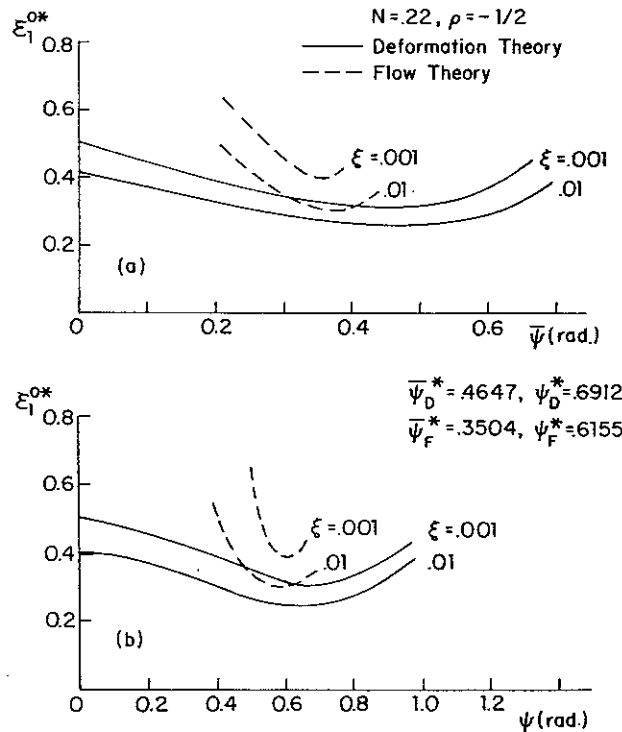


Fig. 7. Limit strain outside neck ϵ_1^{0*} as a function of necking band orientation for two plasticity theories: (a) in terms of initial orientation angle $\bar{\psi}$, (b) in terms of final orientation angle ψ^* . (Numerical values of ψ^* give corresponding values from bifurcation analysis.)

tions as large as analyses give rea-

Forming limit c for an imperfect .50. In the negat resemble the rela. Consequently, the just shift the form

The flow theory K [14] analysis, v ized necking. In rises much more theory curve. Fu steeply, whereas increases.

Although it is c theory and exper in Fig. 8 and relat such as strain-rat pertinent in an e:



Fig. 8. Compa hardening levels f
References pp. 14

tions as large as $\xi = .01$ the critical values of $\bar{\psi}$ and ψ from the bifurcation analyses give reasonable estimates for the minimum limit strain.

Forming limit curves, similar to those depicted in Fig. 2, are plotted in Fig. 8 for an imperfection level $\xi = .01$ and for strain hardening constants $N = .22$, $.50$. In the negative ρ range, the shapes of the forming limit curves strongly resemble the related bifurcation limit curves of Fig. 2(a). A similar strong resemblance is also evident in the positive ρ range for the deformation theory results. Consequently, the effect of an initial imperfection in these cases is to essentially just shift the forming limit curves downwards.

The flow theory results in Fig. 8 for $\rho \geq 0$ are representative of the original M-K [14] analysis, where an initial nonuniformity was postulated to describe localized necking. In this biaxial tension range, the flow theory curve for $N = .22$ rises much more steeply with increasing ρ than the corresponding deformation theory curve. Furthermore, for $N = .50$ the flow theory curve also rises fairly steeply, whereas the deformation theory forming limit curve falls slightly as ρ increases.

Although it is difficult at this stage to make quantitative comparisons between theory and experiment, we shall nevertheless comment on the trends predicted in Fig. 8 and related test data. It must be emphasized, however, that many factors such as strain-rate sensitivity, anisotropy and nonhomogeneous straining may be pertinent in an experiment and that such effects have not been accounted for in

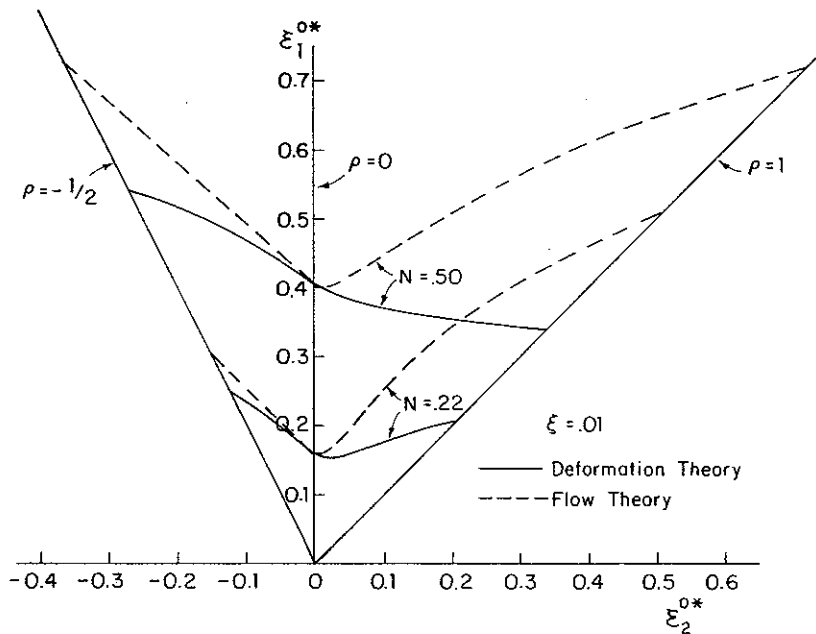


Fig. 8. Comparison of forming limit curves from two plasticity theories at two strain hardening levels for an imperfection $\xi = .01$.

References pp. 149-150.

the present analysis. Furthermore, the testing technique undoubtedly has an important effect on the experimentally-determined forming limit curve [18].

First we note that, in the negative ρ range, it is generally accepted that Hill's predicted curve (31) describes the trend of experiments for materials having lower N -values ($\sim .25$) [19-21]. In this case the flow theory and deformation theory predictions of Figs. 5 and 8 do not differ substantially. However, for materials with higher N -values ($\sim .50$) the discrepancy between the two plasticity theories becomes more pronounced. It is in this range that Painter and Pearce [21] have reported a poor agreement between Hill's curve and test results. In fact, the shape of their experimental curve for brass is very similar to the deformation theory curve in Fig. 8.

Another case where the results of both plasticity theories differ is in the prediction of the band angle at necking (Fig. 7) for a strip under uniaxial tension ($\rho = -\frac{1}{2}$). We simply observe here that, in view of the relative insensitivity of limit strain to variations in groove orientation with deformation theory, this theory would tend to better accommodate any experimental results for which the groove angle may be sufficiently different from the bifurcation prediction. However, available experimental evidence in this respect appears at present to be inconclusive.

In the biaxial tension range ($\rho \geq 0$), forming limit curves for reasonably isotropic metals with lower N -values ($< .25$) have been reported in [4, 18-22]. The experimental trend for these materials is such that the limit strain ϵ_1^0 increases as ρ varies from plane strain to equibiaxial tension. This is in accordance with both theoretical curves in Fig. 8 for $N = .22$. However, the rate of increase observed experimentally tends to be less than that described by the flow theory curve and more representative of the deformation theory predictions. The reported forming limit curves for higher N -values ($> .50$) lend further support to the predictions of deformation theory. In this case the results of Azrin and Backofen [4] for brass and stainless steel, as well as those of Painter and Pearce [21] for brass, show a limit curve which is virtually horizontal or decreases slightly with increasing biaxiality. Only the deformation theory predictions in Figs. 5 and 8 for $N = .50$ indicate this tendency. Even by incorporating other characteristic values of ξ in the analysis, it is doubtful that flow theory can adequately predict this trend.

Throughout our analysis, the quantity ξ defined by (33) is referred to as a geometric nonuniformity. However, as discussed in [14], a material nonhomogeneity can easily be accommodated in the analysis. For example, if the constant K in (11) has values K^0 and K in the uniform section and groove, respectively, then in (40) and the subsequent analysis we need only replace ξ by a new parameter

$$\bar{\xi} = 1 - \frac{K}{K^0} (1 - \xi) \quad (77)$$

which incorporates *both* material inhomogeneity and geometric nonuniformity. It has been suggested [23] that, whereas realistic levels of geometric imperfection do not appear sufficient to bring the flow theory trends in line with experiments,

it might be possible to account for structural metal of ξ .

In summary, the theory, based on localized necking, is not restricted to a particular ρ ($\rho \epsilon_1^0$) so that, the theory give distinctively noncharacterized by used under whether either adequate combined analyses histories.

ACKNOWLEDGMENTS

The work of Research under Grant ENG76-University. The work The support of is gratefully ac

REFERENCES

- [1] R. Hill, J. M.
- [2] Z. Marciniak
- [3] R. Sowerby :
- [4] M. Azrin and
- [5] S. Stören and
- [6] J. W. Hutchi
- [7] R. Hill, J. M
- [8] J. W. Hutchi
ASME (1973
- [9] R. M. McMe
- [10] R. Hill, Proc
- [11] R. Hill, J. M

it might be possible to justify using higher values of $\bar{\xi}$ by appealing to material nonhomogeneities and thereby gain better agreement. For the purpose of discussion of this point suppose that $\bar{\xi} = .01$ and $\xi = 0$, corresponding to a geometrically perfect sheet with a one percent variation in the material parameter K . From (11), this implies a one percent difference in *stress* at any given strain level. It is unlikely that pre-existing nonhomogeneous work hardening levels alone could account for substantially larger stress differences than this at the higher strain levels associated with necking. On the other hand, pre-existing variations in structural metallurgical properties might justify use of substantially larger values of $\bar{\xi}$.

In summary, we are led to tentatively conclude that it is unlikely that a flow theory, based on a smooth yield surface, can be used to adequately predict localized necking in the range $\rho > 0$. This has disturbing implications for the numerical analysis of sheet metal forming. The study in the present paper was restricted to cases in which the overall straining was proportional (i.e., $\epsilon_2^o = \rho \epsilon_1^o$) so that, in the uniform sections of the sheet, deformation theory and flow theory give identical predictions. In extensions to forming histories which are distinctly nonproportional, it is clear that a deformation theory will not adequately characterize behavior in the uniform sections and consequently cannot be reliably used under such circumstances to analyze necking. It appears to us doubtful whether either the deformation theory or the flow theory used here would be an adequate constitutive law for incorporation in a numerical program for the *combined* analyses of overall stretching and localized necking under general overall histories.

ACKNOWLEDGMENT

The work of J.W.H. was supported in part by the Air Force Office of Scientific Research under Grant AFOSR 77-3330, the National Science Foundation under Grant ENG76-04019, and by the Division of Applied Sciences, Harvard University. The work was conducted while K.W.N. was on leave at Harvard University. The support of the Faculty of Applied Sciences at the University of Sherbrooke is gratefully acknowledged.

REFERENCES

- [1] R. Hill, *J. Mech. Phys. Solids*, *1* (1952), 19.
- [2] Z. Marciniak and K. Kuczyński, *Int. J. Mech. Sci.*, *9* (1967), 609.
- [3] R. Sowerby and J. L. Duncan, *Int. J. Mech. Sci.*, *13* (1971), 217.
- [4] M. Azrin and W. A. Backofen, *Metall. Trans.*, *1* (1970), 2857.
- [5] S. Stören and J. R. Rice, *J. Mech. Phys. Solids*, *23* (1975), 421.
- [6] J. W. Hutchinson, *Adv. Appl. Mech.*, *14* (1974), 67.
- [7] R. Hill, *J. Mech. Phys. Solids*, *6* (1958), 236.
- [8] J. W. Hutchinson, *Numerical Solution of Nonlinear Structural Problems* (ed. R. F. Hartung) ASME (1973), 17.
- [9] R. M. McMeeking and J. R. Rice, *Int. J. Solids Struct.*, *11* (1975), 601.
- [10] R. Hill, *Proc. R. Soc. Lond. A*, *314* (1970), 457.
- [11] R. Hill, *J. Mech. Phys. Solids*, *16* (1968), 229, 315.

- [12] R. W. Ogden, *Proc. R. Soc. Lond. A*, 326 (1972), 565.
 [13] R. Hill and J. W. Hutchinson, *J. Mech. Phys. Solids*, 23 (1975), 239.
 [14] Z. Marciniak, K. Kuczyński and T. Pokora, *Int. J. Mech. Sci.*, 15 (1973), 789.
 [15] A. K. Ghosh, *Metall. Trans.*, 5 (1974), 1607.
 [16] J. W. Hutchinson and K. W. Neale, *Acta Met.*, 25 (1977), 839.
 [17] J. W. Hutchinson and W. T. Koiter, *Appl. Mech. Rev.*, 23 (1970), 1353.
 [18] A. K. Ghosh and S. S. Hecker, *Metall. Trans.*, 5 (1974), 2161.
 [19] S. S. Hecker, *Sheet Metal Ind.*, (1975), 671.
 [20] S. S. Hecker, *J. Eng. Mater. Technol. (Trans. ASME, H)*, 97 (1975), 66.
 [21] M. J. Painter and R. Pearce, *J. Phys. D: Appl. Phys.*, 7 (1974), 992.
 [22] R. Venter, W. Johnson and M. C. de Malherbe, *Int. J. Mech. Sci.*, 13 (1971), 299.
 [23] A. Needleman, *J. Mech. Phys. Solids*, 24 (1976), 339.

DISCUSSION

S. Nemat-Nasser (*Northwestern University*)

One thing I was wondering if you'd like to make a comment on. The approach is essentially macroscopic which is certainly what one expects to have eventually, but it seems to me that microstructure must play quite a significant role in the whole process, and I did not see you emphasizing that.

Hutchinson

Hopefully, the role of the microstructure is reflected by the macroscopic law. More complex constitutive laws may be used than what I have discussed here. As an example, recently Needleman and one of his graduate students at Brown University have used a phenomenological characterization of the effect of void growth on yield behavior. So that is a microstructural effect which they have incorporated in the yield surface behavior. I think there will be some discussions on this tomorrow when Jim Rice talks. Now I might also add that when I said you could not use flow theory with a smooth yield surface, I did not mean to rule out that by doing something such as this one indeed might get around the problems associated with a smooth yield surface.

A. K. Ghosh (*Rockwell International*)

I have the following comment. You tended to reject the flow theory on the basis of the fact that it predicts too high a limit strain on the positive ($\epsilon_2 > 0$) side. Now professor Marciniak has made measurements of fracture strain for a number of materials, and I have done some of that type of work as well. It seems that near the balanced biaxial end of the forming limit diagram you do have fracture influencing formability, and even though flow theory predicts a high limit, flow will be terminated by fracture. So, I feel that the fact that the fracture limit comes down into the balanced biaxial end may be the controlling factor. Therefore, there is no arbitrary reason to throw out flow theory.

That's one point, with respect to the Hill's new yield criterion up on the positive uniaxial strength. It be wrong.

Hutchinson

Based on both A that, for example v which suggests that and, therefore, you iments were showin for this new 3-par pendence but the p σ_b over σ_u . Now, I generally speaking biaxial region, whi

Ghosh

I am thinking o goes with its $X >$ which has an X le

Hutchinson

Well, maybe M

P. B. Mellor (*Uni*)

I'd just like to in fact Hill's new Marciniak-Kuczy matically at bala ever assumed. W are plenty of voi density changes making is to inc down.

Hutchinson

And you are 1

That's one point, and the second point—I didn't quite understand one aspect with respect to the calculations. You have shown the m effect (parameter in Hill's new yield criterion): for biaxial strength less than uniaxial the FLD goes up on the positive side, and it comes down for biaxial strength greater than uniaxial strength. I thought the experimental evidence was to the contrary. I may be wrong.

Hutchinson

Based on both Miyauchi's paper and that of Mellor, my understanding was that, for example with Mellor's material, he was seeing relatively low r values which suggests that if you used Hill's old formula the biaxial yield stress was low and, therefore, you get more strengthening in that biaxial region. But the experiments were showing the opposite. Well, that's consistent with the trends I show for this new 3-parameter yield surface. It essentially decouples their interdependence but the predominant effect is the effect of m , that is to say the ratio of σ_b over σ_u . Now, I asked Dr. Miyauchi just after lunch and he also verified that, generally speaking, when his X -parameter decreases you get more strain in the biaxial region, which is consistent.

Ghosh

I am thinking of steel versus brass. Steel shows a rising forming limit which goes with its $X > 1$, brass with a line not rising, independent of strain state, which has an X less than one.

Hutchinson

Well, maybe Mellor wants to comment on this.


P. B. Mellor (*University of Bradford, U.K.*)

I'd just like to question as well that on the biaxial tension quadrant, we have in fact Hill's new yield criterion for aluminum and for brass. If we put that into Marciniak-Kuczyński theory, we find that this brings down the limit strain dramatically at balanced biaxial tension, by an amount far more than I would have ever assumed. We find no cause to call for a fracture theory. One knows if there are plenty of voids then there is going to be fracture. So we have measured the density changes and we find these to be very, very small. Well, the point I am making is to incorporate the m value in the M-K theory brings the strains right down.

Hutchinson

And you are talking about $m < 2$?

Mellor

Surely yes. 

Hutchinson

So that's completely consistent and you have helped to answer the first of Ghosh's questions too. I have no doubt that using Hill's new yield criterion in conjunction with the M-K analysis will also lead to the same trends. I am sure of it. And you can see from Mellor's comments that the trend is in the right direction. With respect to your first remark, I am sure there are materials in biaxial tension which may indeed fracture before significant strain localization occurs. I don't question it. But, I suspect that that's not the general case. And so, if you have to justify the Marciniak analysis based on flow theory and if you always have to invoke a fracture strain, then you start to worry about the theory. Can I say just a little bit more? It shouldn't be a surprise that flow theory overestimates things. You know, in plastic buckling, where we are not nearly as far into the plastic range, it has been known for 20 years, that if you use flow theory, certainly in a bifurcation analysis, you are going to overestimate the buckling load. All the engineering formulas for plates and shells based on bifurcation analysis use deformation theory moduli. Now it is also true, I believe, that most people think that if you do incorporate imperfection in a buckling calculation, with flow theory, you certainly do get much more realistic predictions. This is still somewhat of an open question. The reason, I think, there is so much more problem in the sheet metal necking is because straining is so much further into the plastic range. The discrepancies are therefore much greater. Again, I emphasize that just from a mathematical point of view I think you have strong reason to question using flow theory with a smooth yield surface, just because there is such enormous imperfection sensitivity which doesn't seem to be present in the data.

Ghosh

Yes, but when you see experimental fracture strain much lower than the predicted strain, you know the sample has fractured much earlier than. . . .

Hutchinson

Agreed. But are you suggesting that's the general case?

Ghosh

Well, in the material that you dealt with, certainly brass and A-K steel in the balanced biaxial end.

Hutchinson

That's not what Mellor said.

SHEET NECKING

P. G. Hodge

I guess I can see that. You made the same under uniaxial tension. You have shown that the same things are the same under external load. They have highly

Hutchinson

I agree.

J. L. Duncan

I'd just like to know what the forming limit shape for the

Hutchinson

I think you

Duncan

Except for the under plane stress, the value in your data. I think in all cases equal or less

Hutchinson

No, that's the other side of that coin

Duncan

I am talking

Hutchinson

Well, then the deformation theory is the answer to the imperfection. The limit strain

P. G. Hodge, Jr. (*University of Minnesota*)

I guess I can quibble about a term here which I am sure you will agree with. You made the comparison of flow and deformation theory being essentially the same under proportional loading. In the case of a test being carried out when you have homogenous stress state, proportional loading and proportional stressing are the same thing. In any application, however, you might have proportional external loading, but because you have a non-homogenous stress state you may have highly non-proportional stressing.

Hutchinson

I agree.

J. L. Duncan (*McMaster University, Canada*)

I'd just like to comment on one point. Given an experimentally determined forming limit curve and a Marciniak analysis, it's possible really to choose a shape for the yield surface that will give you a fit.

Hutchinson

I think you are probably right on that.

Duncan

Except for some degree of difficulty and that is, when the forming limit strain under plane strain conditions exceeds the strain hardening index value, the N value in your notation. I wonder whether you can comment on this point, because I think in all of your diagrams the forming limit strain that you measured was equal or less than the strain hardening index, N , at the plane strain axis.

Hutchinson

No, that's not really true. It's true at the higher N values on the right hand side of that diagram.

Duncan

I am talking about the plane strain axis, where $\epsilon_2 = 0$.

Hutchinson

Well, then I should say that there is no issue in plane strain, because the deformation theory and the flow theory coincide in all calculations. But, I think the answer to your question is, if it's perfect and if you don't introduce an imperfection, then the necking does occur at N . If you introduce an imperfection, the limit strain is reduced fairly substantially as Neale will discuss tomorrow.